HLS

Lunar Surface Crater Thermal Effects on Lander Radiator Performance

Will Grier (LaRC-D206*)
Will Birmingham (MSFC-EV34**)
Lisa Erickson (JSC-EC611***)
Tai Valdés (LaRC-D206*)

05/06/26

*Engineering Directorate - Structural and Thermal Systems Branch
**Spacecraft and Vehicle Systems Department - Thermal Analysis and Control Branch
***Crew and Thermal Systems Division - Thermal Systems Branch

Content

- Study Purpose
- Model Overview
  - Lunar Thermal Environment
  - Lander Submodel
  - Flat Surface Submodel
  - Crater Surface Submodel
- Results
- Findings
- References

Study Purpose

Problem Statement: Lunar surface craters smaller than the spatial resolution of surface meshes used in typical Lunar surface thermal models (10 to 60 meters per pixel) may impact the accuracy of thermal model extrema predictions for Landers.

Study Goal: Investigate the thermal sensitivity of representative lander systems with realistic thermal surface orientations in bare and cratered terrain environments at relevant Artemis mission locations

Summary: This thermal analysis task investigates the impact of lunar surface craters on lander radiator performance by comparing heat rejection capability results between bare and cratered terrain environments. This study examines external body-mounted lander radiator thermal performance across varying lander heights (5.5m, 20m, 50m) and radiator orientations (horizontal, 45º tilted, and vertical) at two representative Artemis mission latitudes (-89.5ºS and -82.5ºS), spanning from the Shackleton Connecting Ridge to Mons Mouton Plateau.

HLS

Model Overview

- **Analyzed 12 total cases;** 2 latitudes x 3 lander heights x 2 ground plane types
  - Latitudes = -89.5ºS, -82.5ºS
    - Range of Artemis sites (Shackleton Ridge to Mons Mouton Plateau)
  - Lander heights = 5.5m, 20m, 50m
  - Flat terrain with craters and without craters
- **Height variable reduced order lander model with three radiator orientations**
  - Representative of existing vehicles in terms of height, optical properties, external surface temperatures, and radiator placement
- **Assumptions:**
  - Assessing only body mounted radiators (single-sided)
  - Not including thermal impacts from far field terrain (mountains, valleys, etc.)[1,2]
  - Max crater diameter of 50m adjacent to landing origin
  - Lander is not placed within a crater

Submodel	Nodes
CRATER_SURFACE	22183
FLAT_SURFACE	1444
RADIATOR_HORIZONTAL	2
RADIATOR_TILTED	16
RADIATOR_VERTICAL	16
STRUCTURE	26

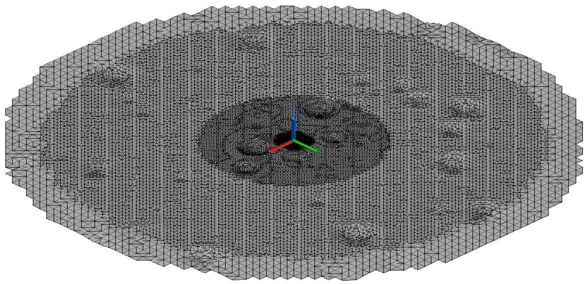

CRATER_SURFACE

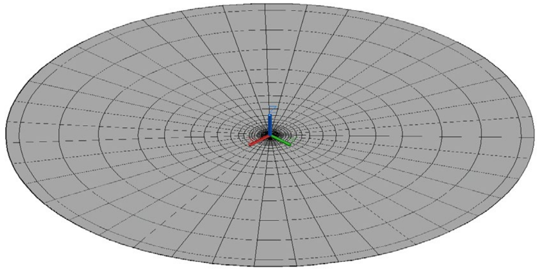

FLAT_SURFACE

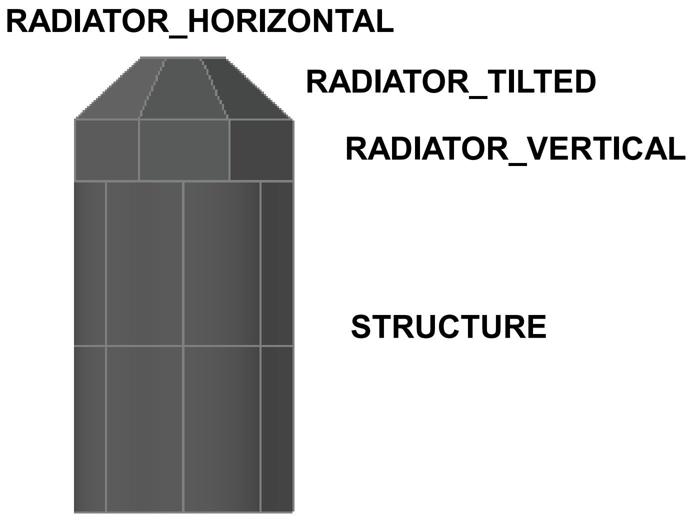

Versions: Thermal Desktop = 6.3 Patch 27, Model = Crater_v1e_WJG

Lunar Thermal Environment

(applied identically for both crater and flat surface submodel runs)

- **Lunar environment defined using the Human Landing System (HLS) Lunar Thermal Analysis Guidebook (LTAG), Design Specification for Natural Environments (DSNE), and JPL Horizons data [3,4,5]**
  - Subsurface layers initialized via 10-year model run[3]
  - Time varying and location dependent solar vector paths[5]
    - Transient runs capture shadowed and illuminated periods
  - Constant worst case hot solar flux of 1415 W/m²
  - Solar diameter (subtended) angle (0.53°)[3]
  - Surface IR emissivity[6] and solar absorptivity[7]
    - Highland directional α_s (polar)[7] (angle dependent)
  - Surface density[8,9] and specific heat[10] (depth dependent)
  - Surface thermal conductivity (depth & temperature dependent)[9]

- **Selected candidate Artemis landing site latitudes**
  - -89.5ºS, Initializer (6/1/16 to 6/1/26), Transient (6/1/26 to 12/9/26)
  - -82.5ºS, Initializer (11/3/16 to 11/3/26), Transient (11/3/26 to 12/16/26)

- **Not included in thermal model**
  - Subsurface ground heat flow (~0.018 W/m²)[11]
  - Impacts from regolith dust deposition onto external surfaces
  - Thermal impacts from far field terrain
  - Earthshine (0 to 0.15 W/m²) and eclipses (~hours)[3]

-89.5ºS Case, Solar Transient

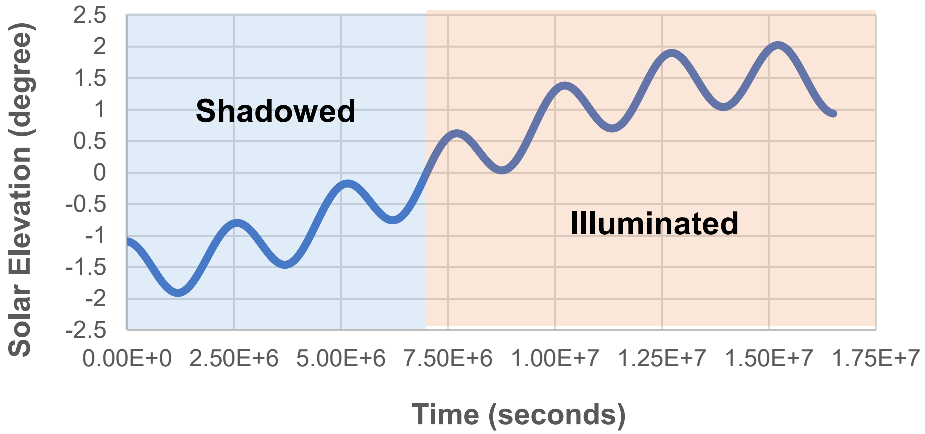

-82.5ºS Case, Solar Transient

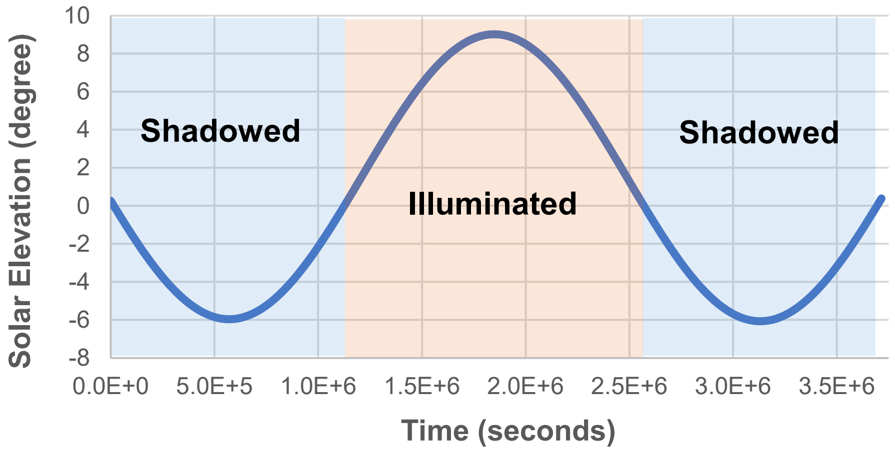

HLS

Caution: B_{ij}/F_{ij} Cutoff Factor

- **Recommendation:** Verify B_{ij}/F_{ij} cutoff factor in Thermal Desktop[tm] for lunar surface thermal models
- Improper B_{ij}/F_{ij} cutoff factor settings cause inaccurate heat rejection predictions by filtering out small (with respect to primarily view factor and emissivity) but important radiation exchange values in high node-count models

- For Lunar surface models where a relatively hot lander is present, an improper value results in hot near-surface contributions dominating calculations while colder far-surface regions are neglected, creating an inaccurate hot environment bias
    - The lander creates localized hot regions on the Lunar surface near the origin of the model
- B_{ij}/F_{ij} cutoff factor ≤ 1 / (10 × node count)
    - For 25,000 nodes: use ≤ 4×10^{-6} (this analysis used 1×10^{-7})
    - For 1,000 nodes: use ≤ 1×10^{-4} (default 1×10^{-3} may be insufficient)

<u>Generalized Lunar Surface Model Temperature Diagram</u>

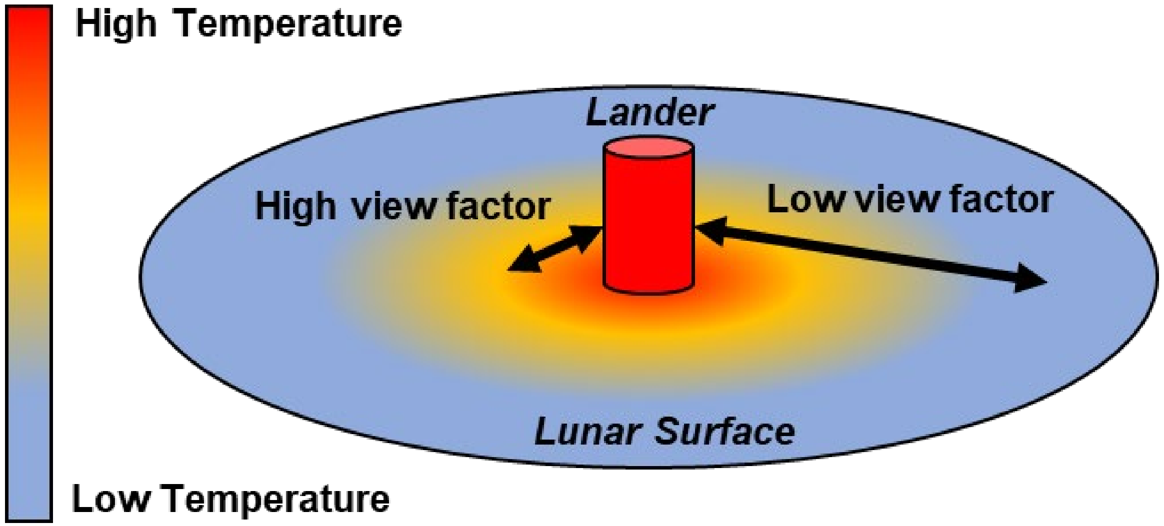

HLS

HLS

Lunar Lander Survey

- **Historical, currently available, and in-development Lunar landers vary in design, size (height), and employ different radiator surface placements and orientations**
  - Three representative lander heights and radiator orientations were selected for inclusion in this study
    - *Lander heights = 5.5m, 20m, 50m; radiator orientations = horizontal, 45º tilted, and vertical*

Firefly Blue Ghost[12]	Intuitive Mach. NOVA-C[13]	Apollo LEM[14]	Blue Origin Mk1[15]	Blue Origin Mk2[16]	SpaceX Starship[16]
Height: ~2m	**~4m**	**~7m**	**~8m**	**~15m**	**~50m**
	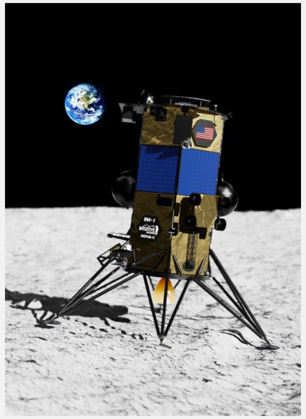	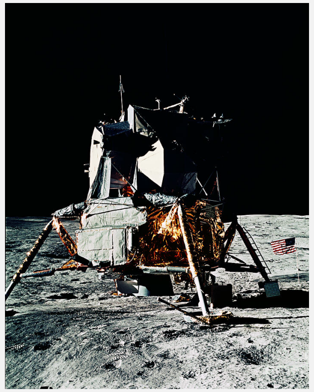			

[12] "Fireflyspace.com, 2025. https://fireflyspace.com/wp-content/uploads/2025/01/BGM1-Component-Graphic-vJan14-2025a.png, [13] "NOVA-C | Intuitive Machines," Intuitive Machines, 2024. https://www.intuitivemachines.com/nova-c, [14] "NASA's Apollo 11 Lunar Module (Basic Facts)," Apollo11Space, Dec. 08, 2019. https://apollo11space.com/nasas-apollo-11-lunar-module-basic-facts/, [15] Wikipedia Contributors, "Blue Moon (spacecraft)," Wikipedia, Nov. 21, 2025., [16] Astralytical, "SpaceX's Starship vs Blue Origin's Blue Moon: Who's landing first?," Substack.com, Mar. 18, 2024. https://astralytical.substack.com/p/spacexs-starship-vs-blue-origins (accessed Nov. 29, 2025).

Lander Submodel

- ***Analyzed three** lander heights (5.5m, 20m, 50m)* **and** *radiator orientations (horizontal, 45º tilted, and vertical)***
- **Reduced order lander model with diffusion node surfaces connected to boundary nodes via conductors**
  - Radiator temperature set at 283K (10ºC) and structure temperature set at 293 K (20ºC)
  - Material set as Al 6061-T6 with all surfaces covered in Z93 (0.16 solar absorptivity, 0.92 IR emissivity)
  - Each radiator surface has an external surface area of 10m²

<u>Lander Dimensions</u>

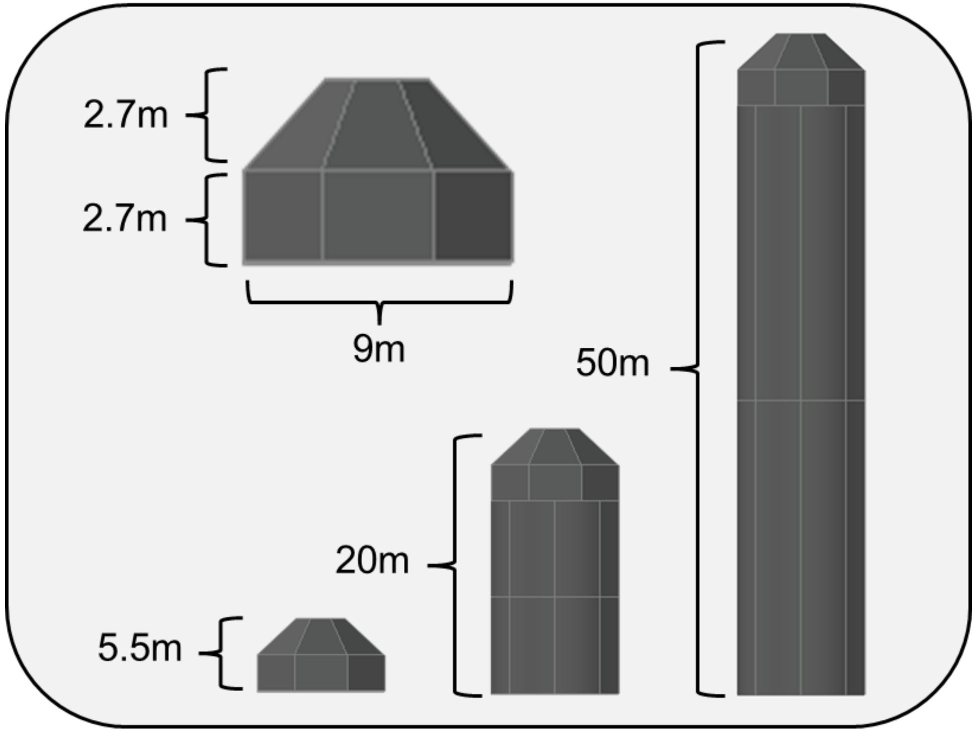

<u>Radiator Node Map & Conductor Diagram</u>

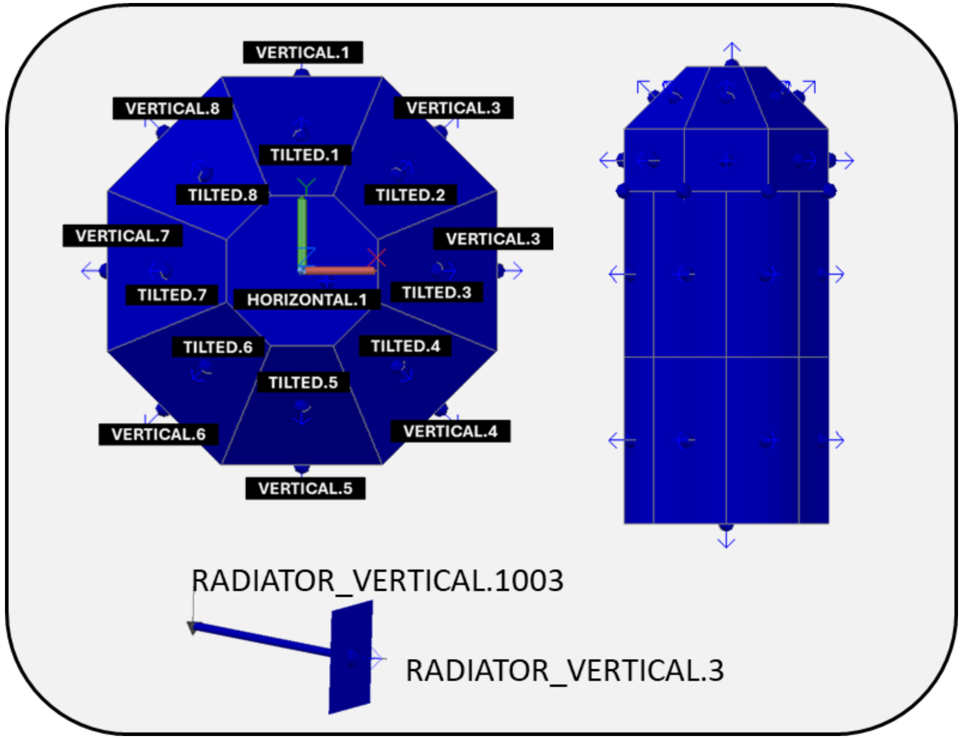

HLS

Flat Surface Submodel

- **Used section 9.3.1.3 "radiant energy: cylinder to ground plane exchange" from the LTAG to size the flat ground plane[3]**
  - Origin ground slope = 0º
  - Max Lander height = 50m
  - Lander radius = 4.5m
  - Surface radius = 325m

Flat Surface Element

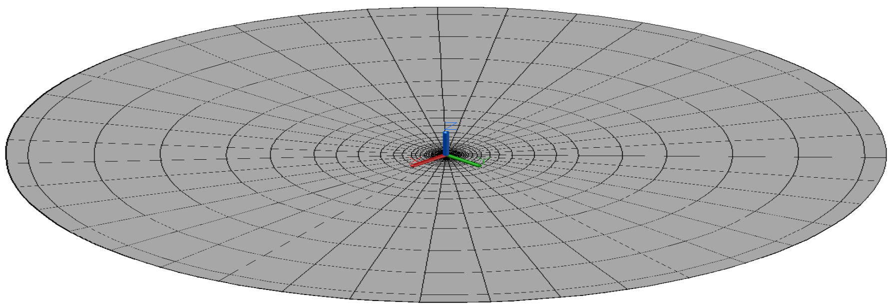

Flat Surface Thermal Result Timestep*

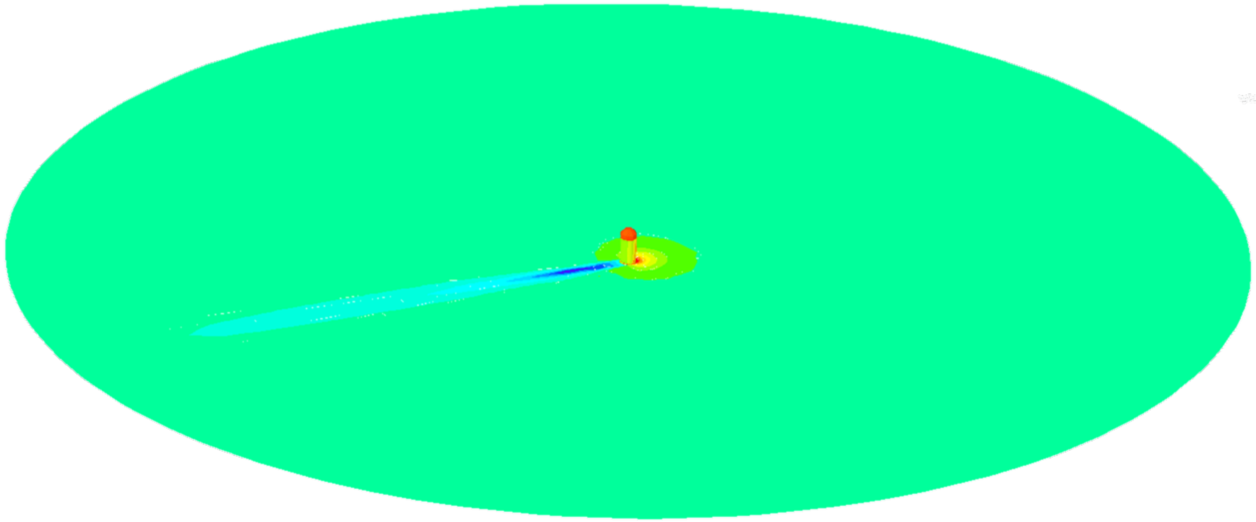

LTAG Section 9.3.1.3[3]

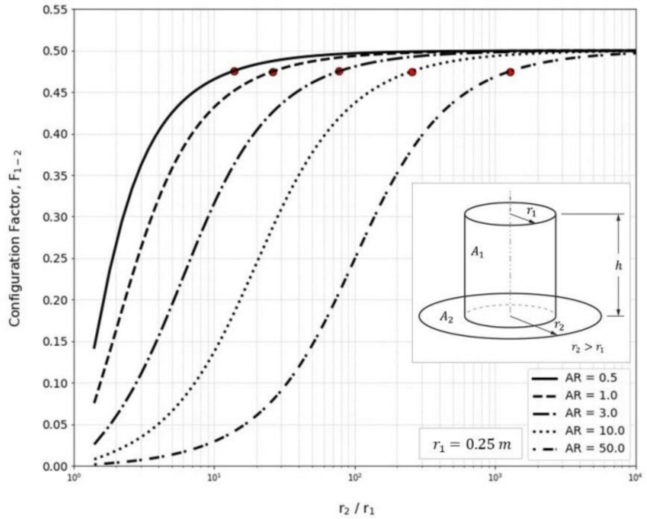

$$(r_2/r_1)_{\Delta 5\%} \cong 12.63(AR) + 0.943$$

*visual only, temperature color scale not provided

Crater Surface Submodel

- **Generated a flat surface mesh with a crater distribution**
  - Origin ground slope = ~1.5º (varies)
    - Influenced by small craters from synthcrater[17-19]
  - Max crater diameter at surveyed Artemis candidate sites = 50m
  - Radius = 325m

Crater Surface Mesh View

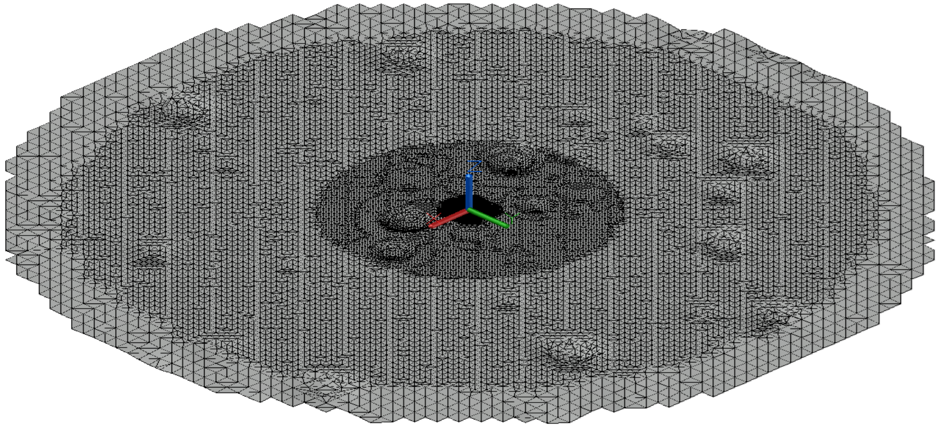

Crater Surface Thermal Result Timestep*

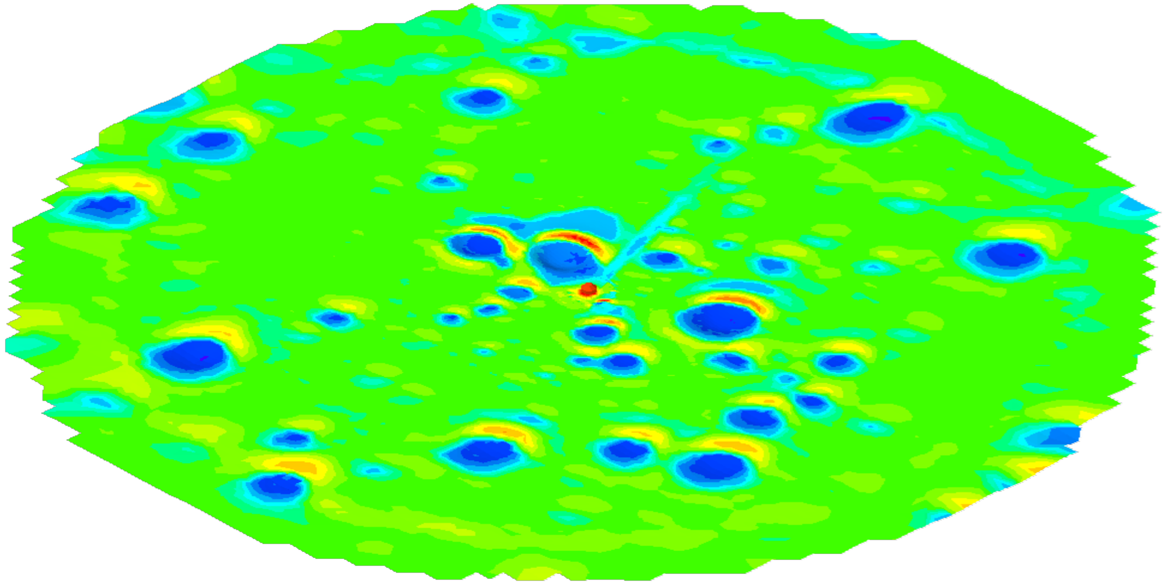

Crater Surface Shaded View

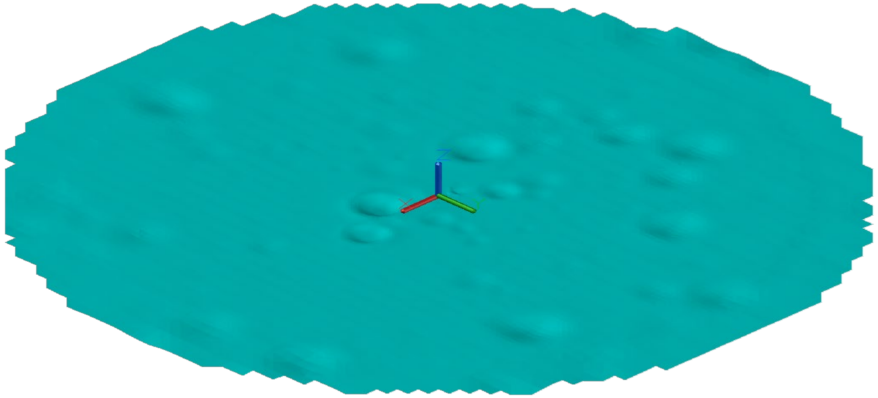

*visual only, temperature color scale not provided

HLS

HLS

Synthetic Crater Distribution Generation

- **Utilized a Lunar Navigation Maps (LuNaMaps) project developed program that generates synthetic crater populations and places them onto a flat point cloud[17-19]**
- The synthcrater program generates craters with realistic diameters, depths, and ages as specified in planetary science literature and NASA's DSNE
  - Craters are embedded in "age order," and each new crater impact considers the previous topography so any coincident or overlapping crater will alter the topography of the underlying crater and terrain

Progressive Crater Degradation[19]

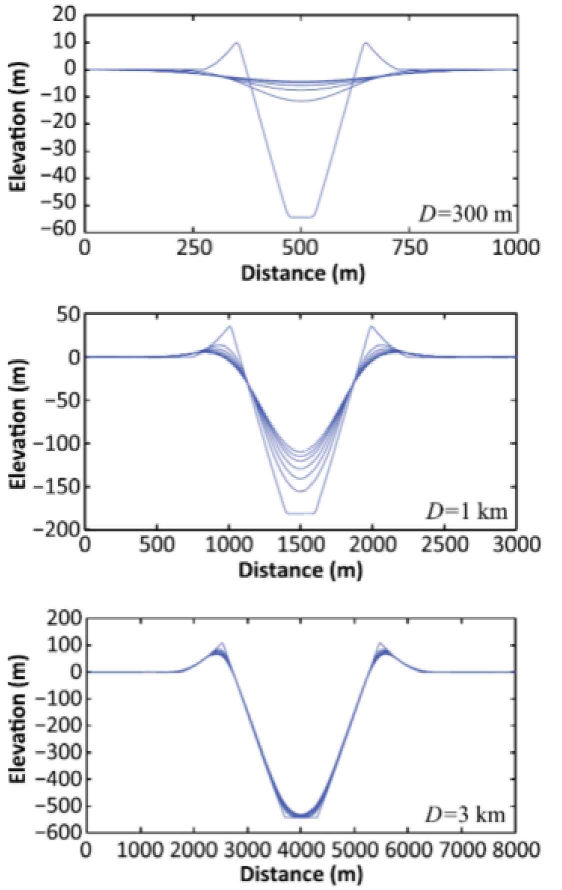

DSNE Crater Distribution Characteristics[4,19]

	Freshest Craters		Degraded Craters		
Fraction of population	0.5%	2.5%	17%	30%	50%
Crater Characteristics	Very steep slopes, pronounced blocks, ejecta, optically immature	Steep slopes, blocks common	Moderate slopes, most blocks on rim	Gentle slopes, rim mostly eroded	Very gentle slopes, no rim
Typical depth/diameter ratio	0.12-0.2+	0.12-0.2	0.1-0.15	0.07-0.1	<0.07
Max. Wall Slope	35°+	25-35°	15-25°	10-15°	<10°

Crater Distribution Results

HLS

- **Synthcrater Input Parameters:**
  - Max crater diameter = 50m
    - Based on inspection of craters inside candidate Artemis landing sites
  - Min crater diameter = 0.5m
  - Point cloud size = 700m x 700m

Crater Diameter vs Depth/Diameter

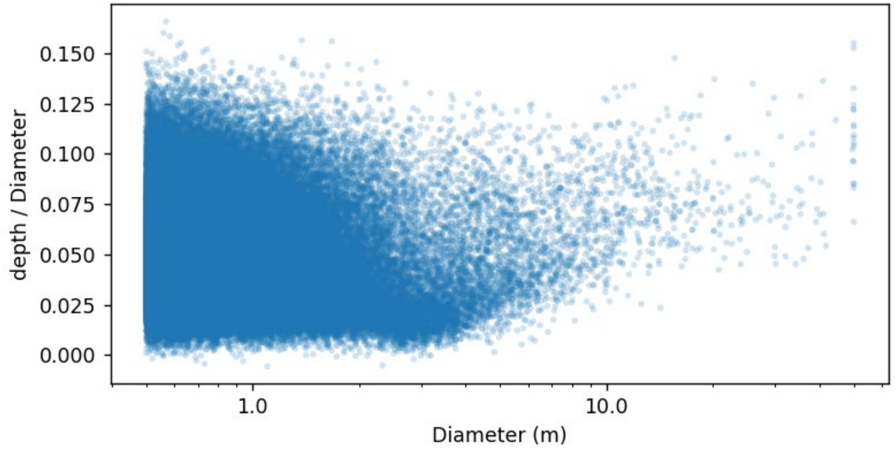

Crater Diameter vs Count

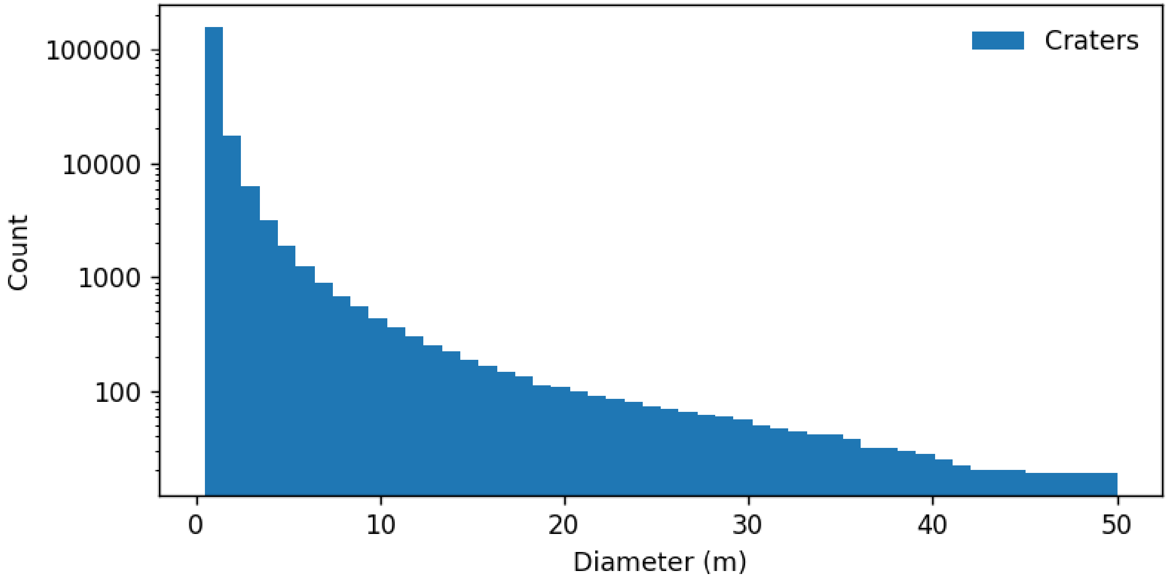

Crater Diameter vs Age

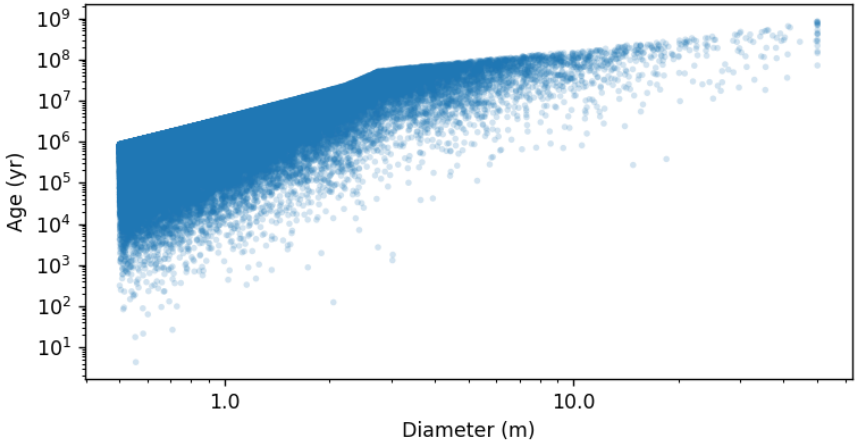

Resulting Crater Spatial Data

- **Converted synthcrater point cloud to a Lunar surface mesh usable by Thermal Desktop**
  - ~0.5 meter per pixel resolution within 15 m from origin, progressively less spatial resolution beyond origin to reduce node count to enable a usable model run time

Synthcrater Point Cloud

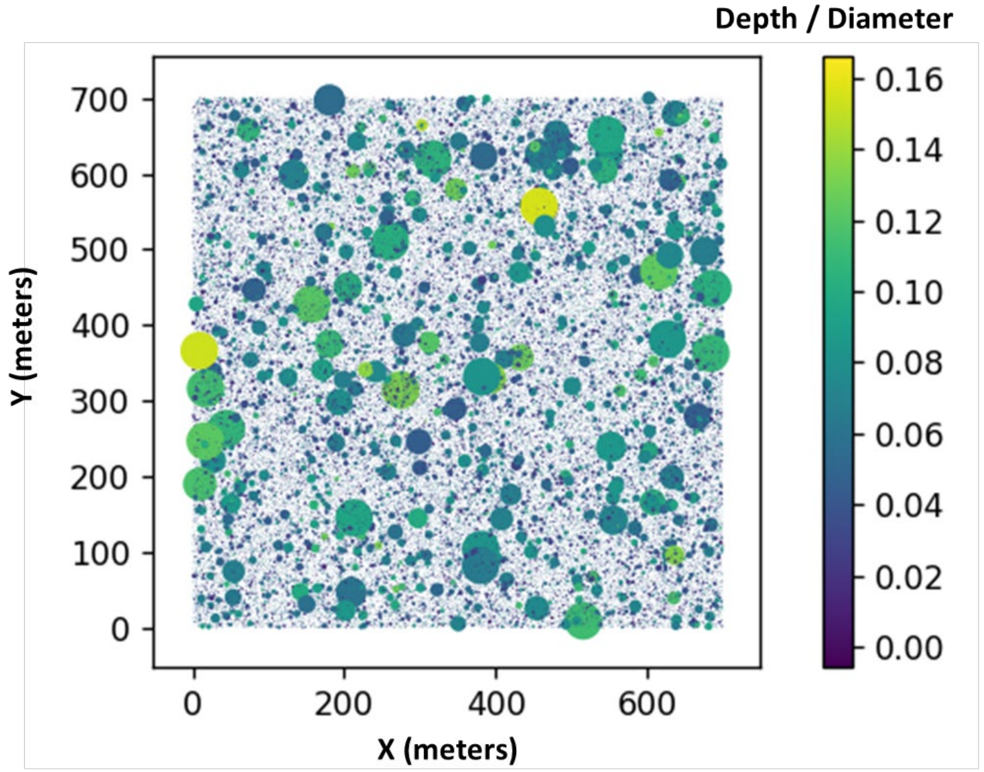

Thermal Model Suface Mesh, Shaded View

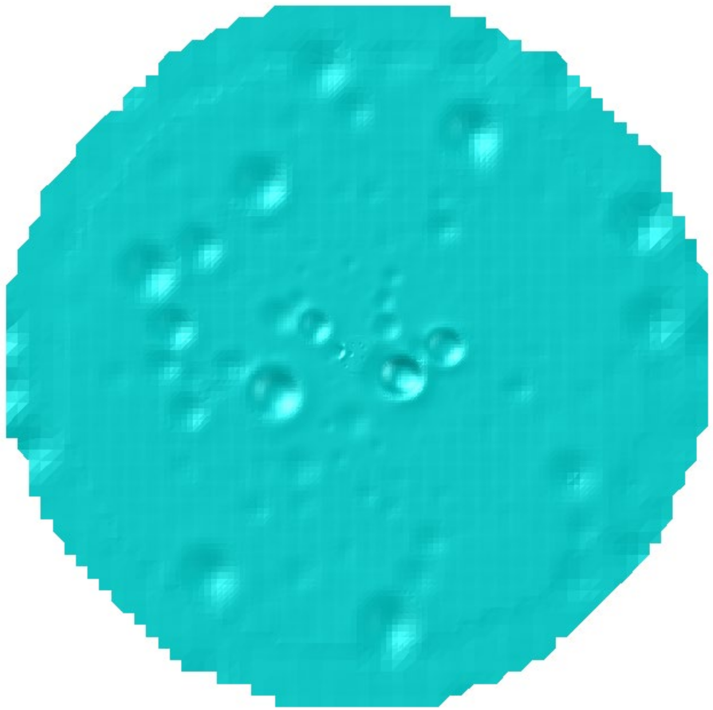

Terrain Modeling Process Overview

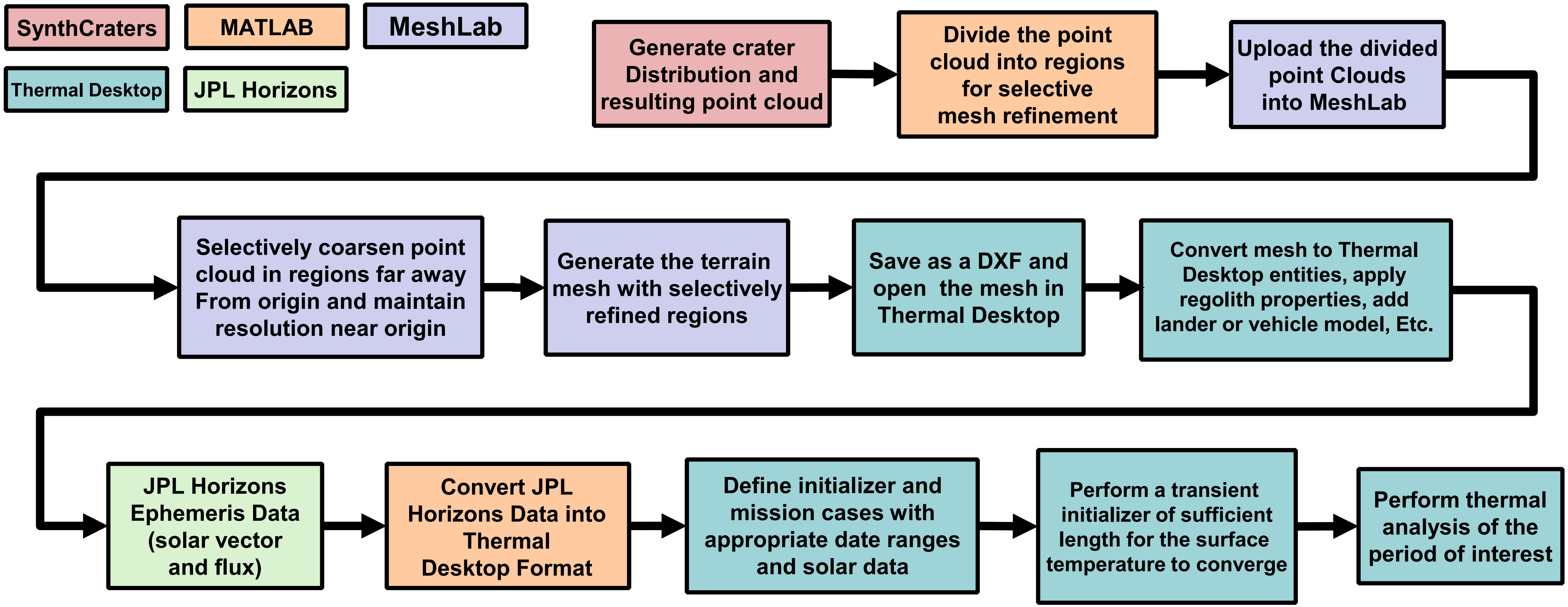

HLS

Results: QFLOW Query

- **Used Thermal Desktop post processing feature QFLOW to query the heat flow from the radiator surfaces to the environment**
- To capture the environmental heating rates incident upon the radiator surfaces in the QFLOW calculations, the input is *from* the internal boundary node *to* the accompanying radiator surface diffusion node
  - Boundary nodes are set at a constant temperature (283 K) and are connected to the radiator surface diffusion nodes via a high conductance conductor (10,000 W/K)

Thermal Radiation Exchange

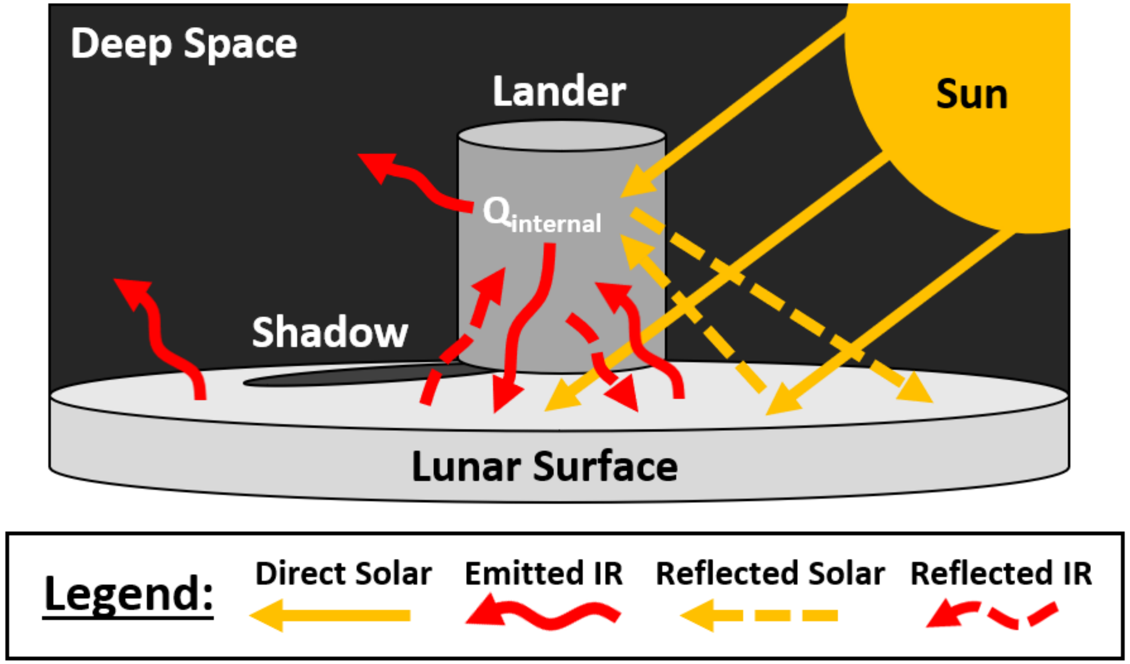

Radiator Nodal Associations

Diffusion Node	Boundary Node
RADIATOR_HORIZONTAL.1	RADIATOR_HORIZONTAL.1000
RADIATOR_TILTED.1	RADIATOR_TILTED.1001
RADIATOR_TILTED.2	RADIATOR_TILTED.1002
RADIATOR_TILTED.3	RADIATOR_TILTED.1003
RADIATOR_TILTED.4	RADIATOR_TILTED.1004
RADIATOR_TILTED.5	RADIATOR_TILTED.1005
RADIATOR_TILTED.6	RADIATOR_TILTED.1006
RADIATOR_TILTED.7	RADIATOR_TILTED.1007
RADIATOR_TILTED.8	RADIATOR_TILTED.1008
RADIATOR_VERTICAL.1	RADIATOR_VERTICAL.1001
RADIATOR_VERTICAL.2	RADIATOR_VERTICAL.1002
RADIATOR_VERTICAL.3	RADIATOR_VERTICAL.1003
RADIATOR_VERTICAL.4	RADIATOR_VERTICAL.1004
RADIATOR_VERTICAL.5	RADIATOR_VERTICAL.1005
RADIATOR_VERTICAL.6	RADIATOR_VERTICAL.1006
RADIATOR_VERTICAL.7	RADIATOR_VERTICAL.1007
RADIATOR_VERTICAL.8	RADIATOR_VERTICAL.1008

Results: -89.5ºS Flat Surface

- **Heat rejection capability trend: *Horizontal* > *Tilted* > *Vertical (orientation) and 50m* > *20m* > *5.5m (height)***
  - Radiator orientation significantly impacts heat rejection capability in the hot case, for cold case performance is similar
  - Radiator height impacts on heat rejection capability are negligible
  - Maximum and minimum heat rejection capability occurs during shadowed (night) and illuminated (day) periods respectively

Delta: Average Heat Rejection (all panels)

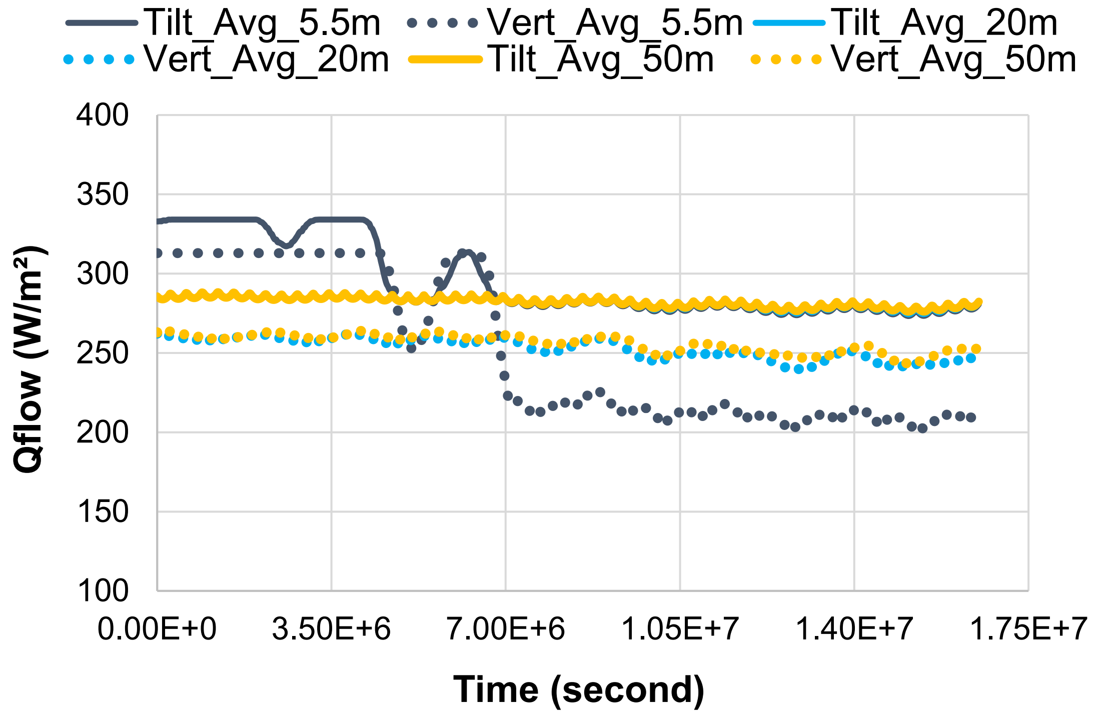

Delta: Max & Min Heat Rejection (single panel)

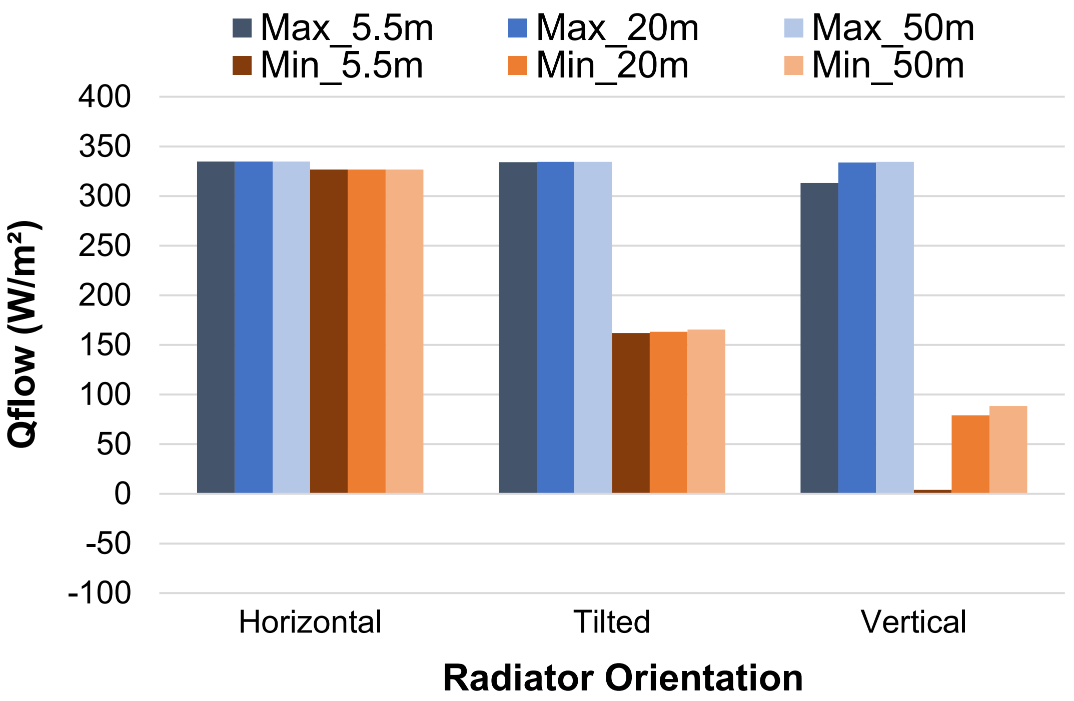

Results: -89.5ºS Crater Surface

- **Heat rejection capability trend: *Horizontal > Tilted > Vertical (orientation) and 50m > 20m > 5.5m (height)***
  - Radiator orientation significantly impacts heat rejection capability in the hot case, for cold case performance is similar
  - Radiator height impacts on heat rejection capability are negligible
  - Maximum and minimum heat rejection capability occurs during shadowed (night) and illuminated (day) periods respectively

Delta: Average Heat Rejection (all panels)

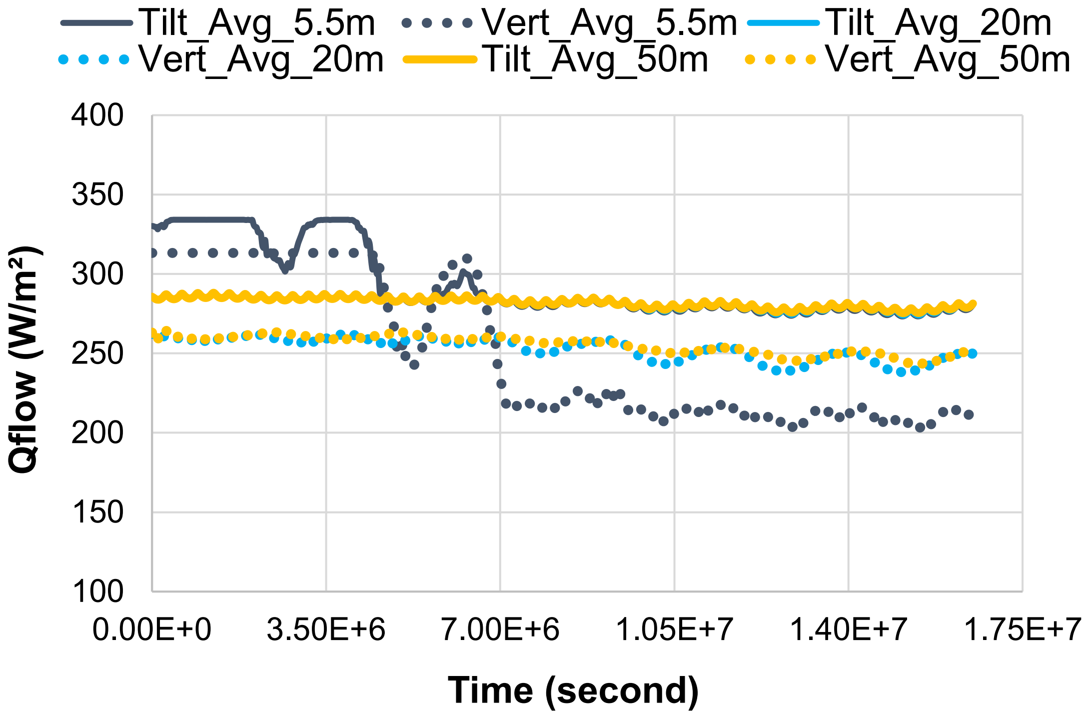

Delta: Max & Min Heat Rejection (single panel)

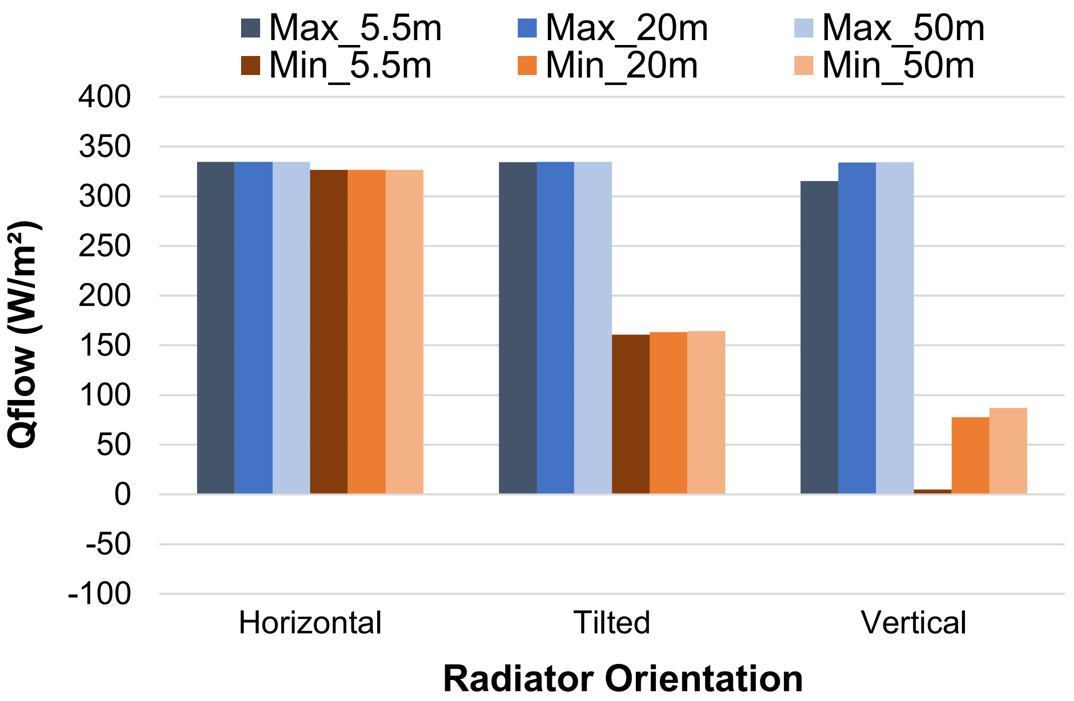

HLS

Results: -82.5ºS Flat Surface

- **Heat rejection capability trend: *Horizontal > Tilted > Vertical (orientation) and 50m > 20m > 5.5m (height)***
  - Radiator orientation significantly impacts heat rejection capability in the hot case, for cold case performance is similar
  - Radiator height impacts on heat rejection capability are negligible
  - Maximum and minimum heat rejection capability occurs during shadowed (night) and illuminated (day) periods respectively

Delta: Average Heat Rejection (all panels)

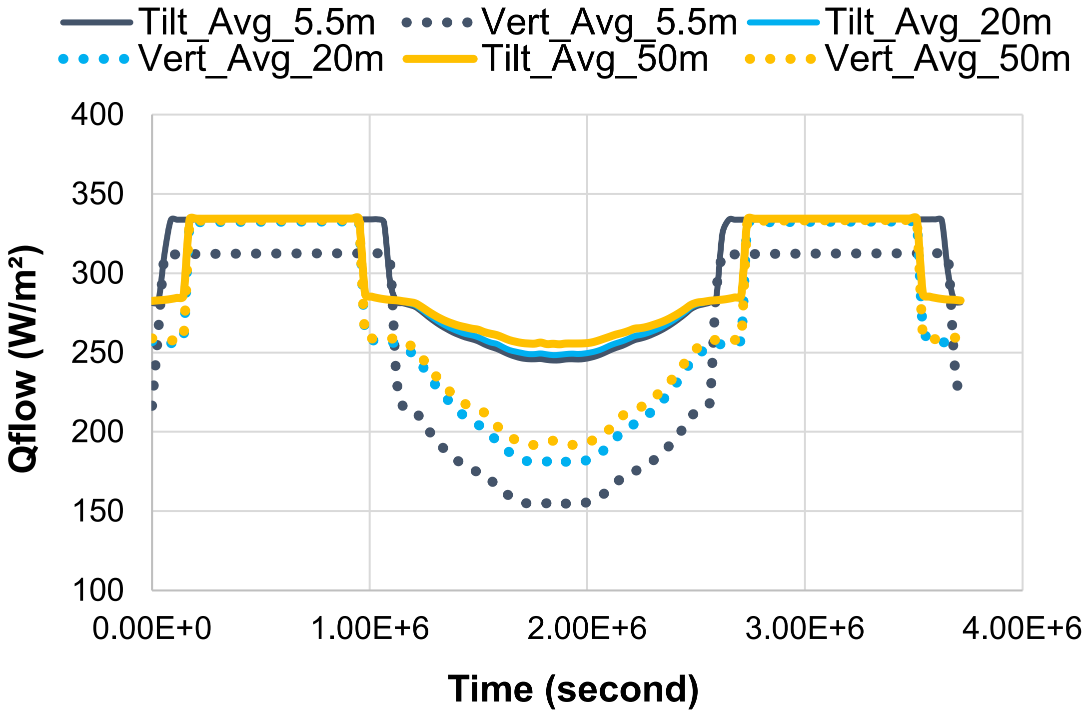

Delta: Max & Min Heat Rejection (single panel)

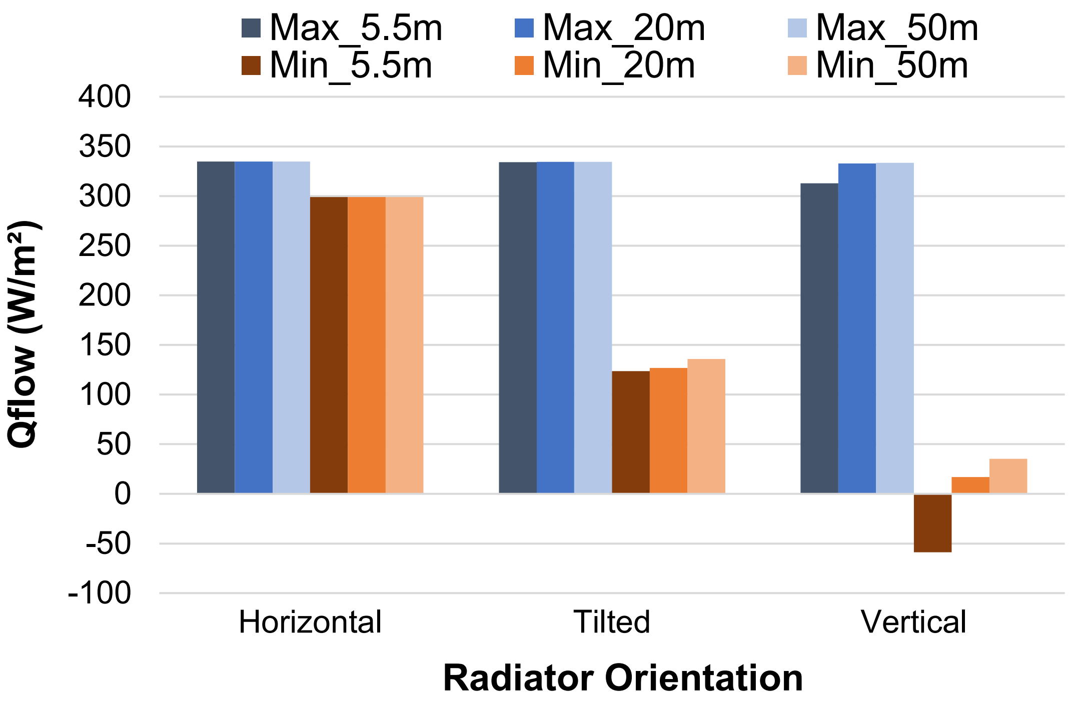

HLS

Results: -82.5ºS Crater Surface

- **Heat rejection capability trend: *Horizontal > Tilted > Vertical (orientation) and 50m > 20m > 5.5m (height)***
  - Radiator orientation significantly impacts heat rejection capability in the hot case, for cold case performance is similar
  - Radiator height impacts on heat rejection capability are negligible
  - Maximum and minimum heat rejection capability occurs during shadowed (night) and illuminated (day) periods respectively

Delta: Average Heat Rejection (all panels)

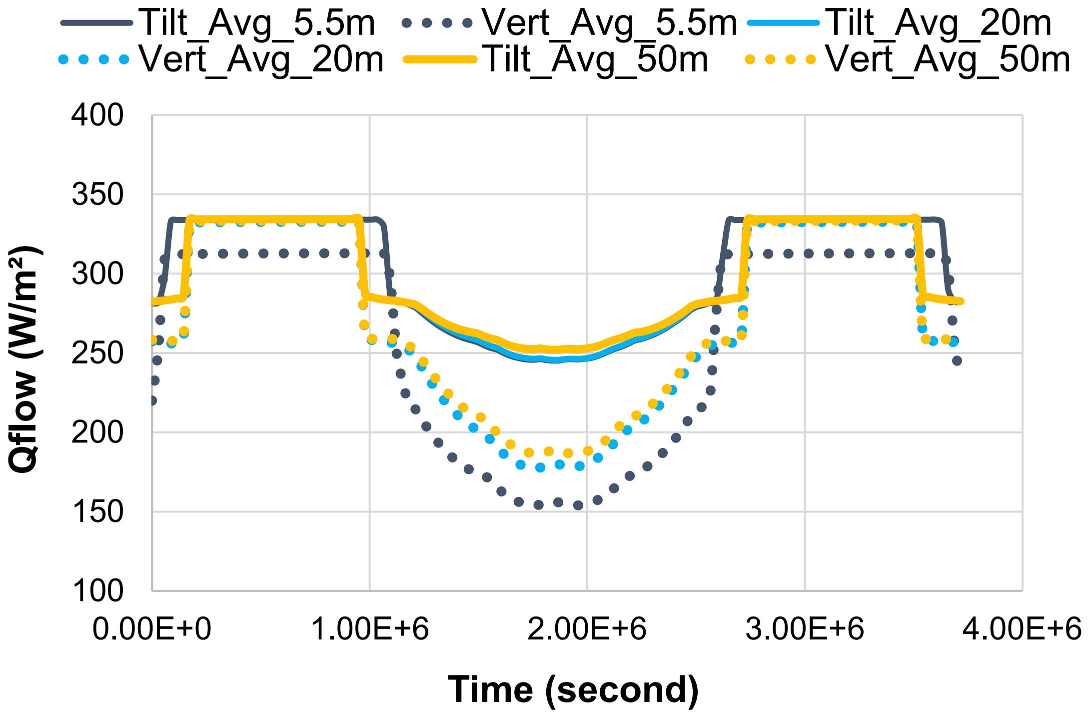

Delta: Max & Min Heat Rejection (single panel)

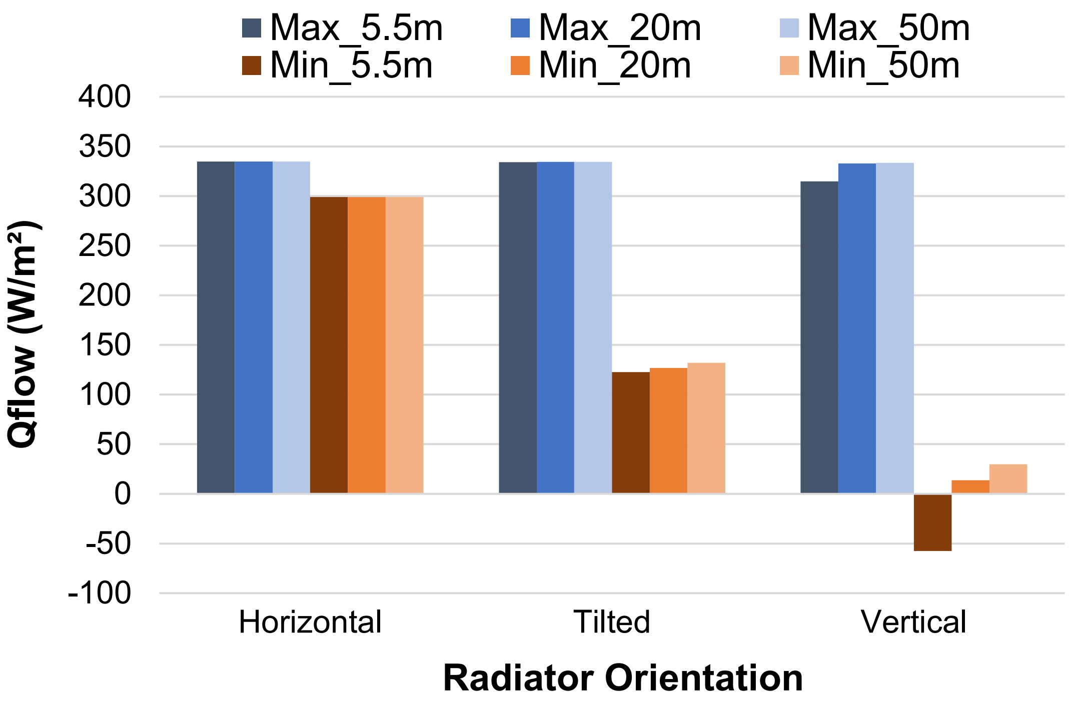

Comparison: -89.5ºS Flat vs Crater

- **When compared to a flat surface, a flat craterous surface presents a near identical thermal environment for a Lunar Lander**
  - Maximum heat rejection for a single radiator panel is 335 W/m^2, single digit variances are negligible
  - Impact magnitude may be different for a smaller and more thermally sensitive asset (e.g., astronaut suit), not analyzed here

$$\Delta Q_{flow} = Q_{flow_{crater}} - Q_{flow_{flat}}$$

Delta: Average Heat Rejection (all panels)

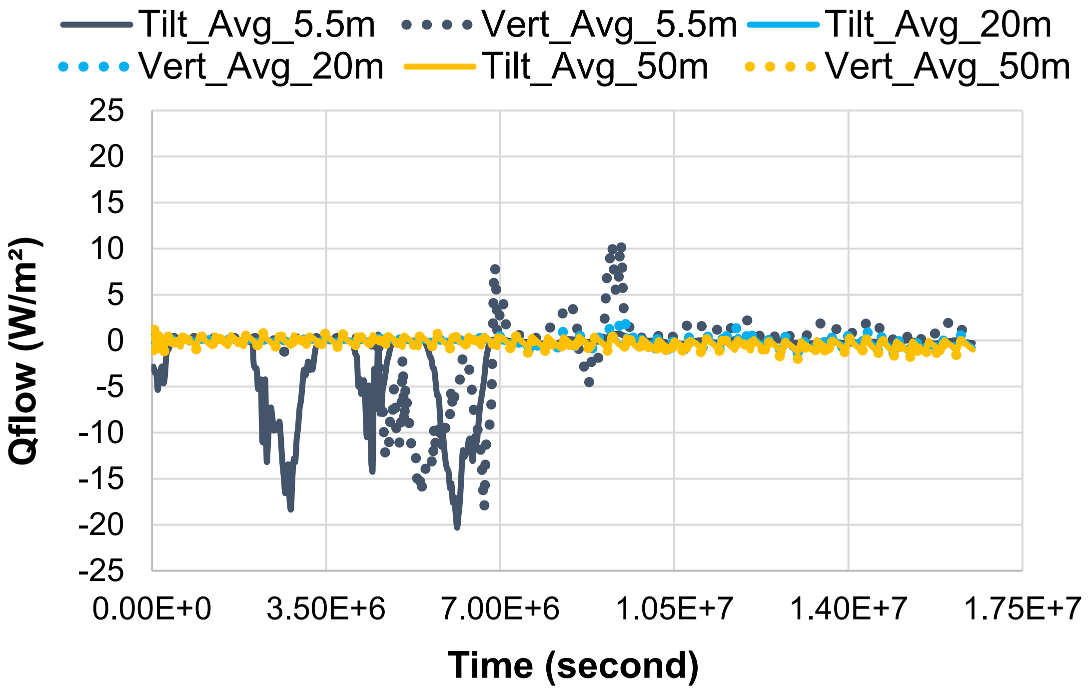

Delta: Max & Min Heat Rejection (single panel)

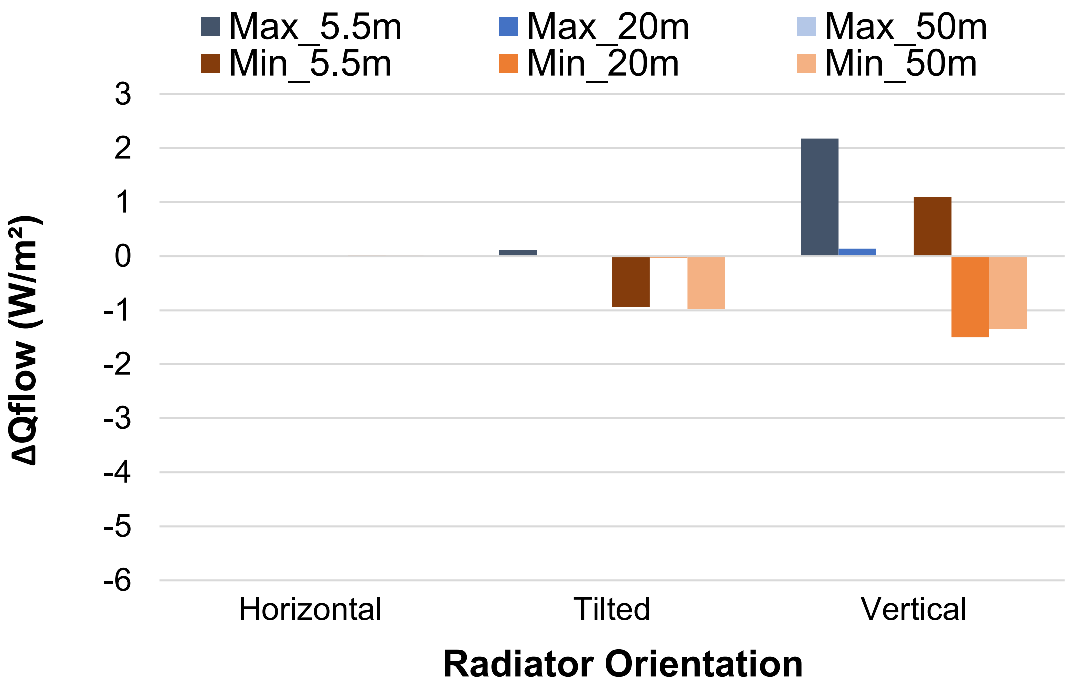

Comparison: -82.5ºS Flat vs Crater

- **When compared to a flat surface, a flat craterous surface presents a near identical thermal environment for a Lunar Lander**
  - Maximum heat rejection for a single radiator panel is 335 W/m^2, single digit variances are negligible
  - Impact magnitude may be different for a smaller and more thermally sensitive asset (e.g., astronaut suit), not analyzed here

$$\Delta Q_{flow} = Q_{flow_{crater}} - Q_{flow_{flat}}$$

Delta: Average Heat Rejection (all panels)

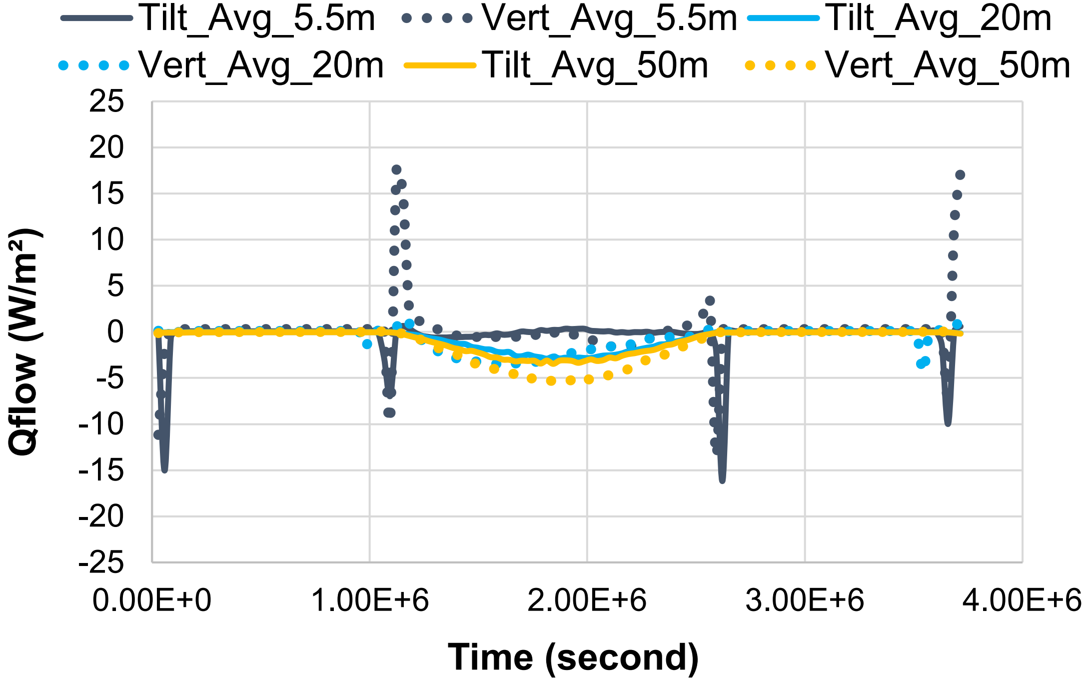

Delta: Max & Min Heat Rejection (single panel)

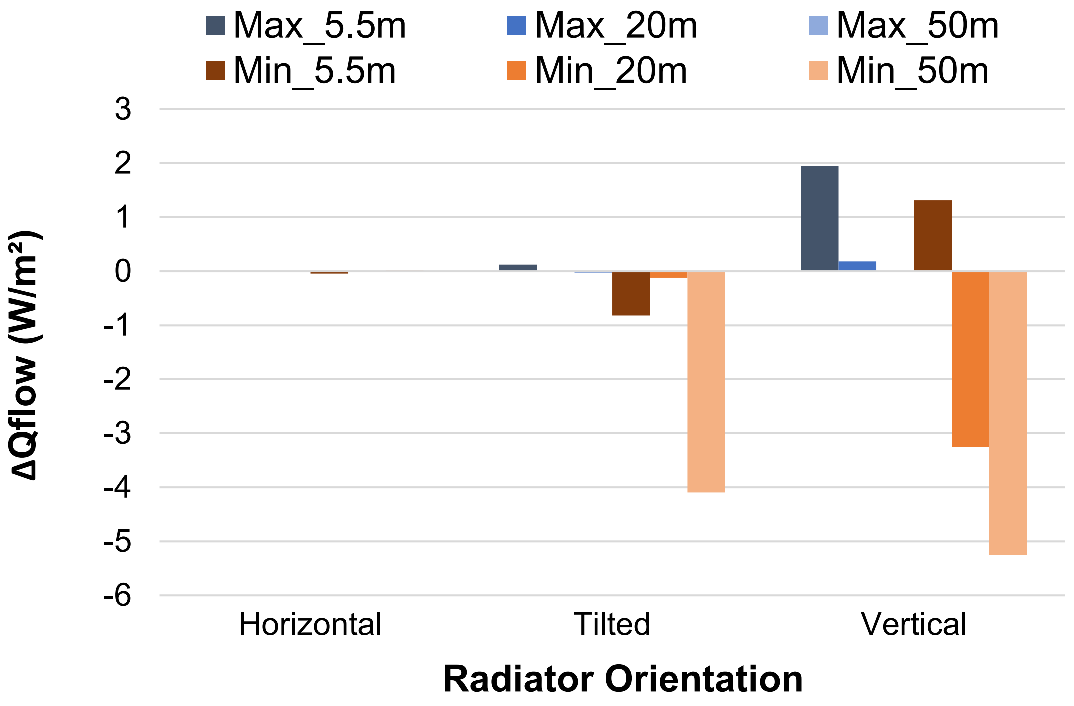

HLS

Comparison: -89.5ºS vs -82.5ºS

- **Observed trends are similar between the compared latitude cases (flat and crater):**
  - Heat rejection capability degrades as latitude increases due to elevated solar angle
  - Minimal capability differences observed between radiator heights vs latitude for titled and vertical orientations

$$(1)\Delta Q_{flow} = Q_{flow_{-82.5°S\_flat}} - Q_{flow_{-89.5°S\_flat}}$$

$$(2)\Delta Q_{flow} = Q_{flow_{-82.5°S\_crater}} - Q_{flow_{-89.5°S\_crater}}$$

(1) Delta: Flat, Max & Min Heat Rejection (single panel)

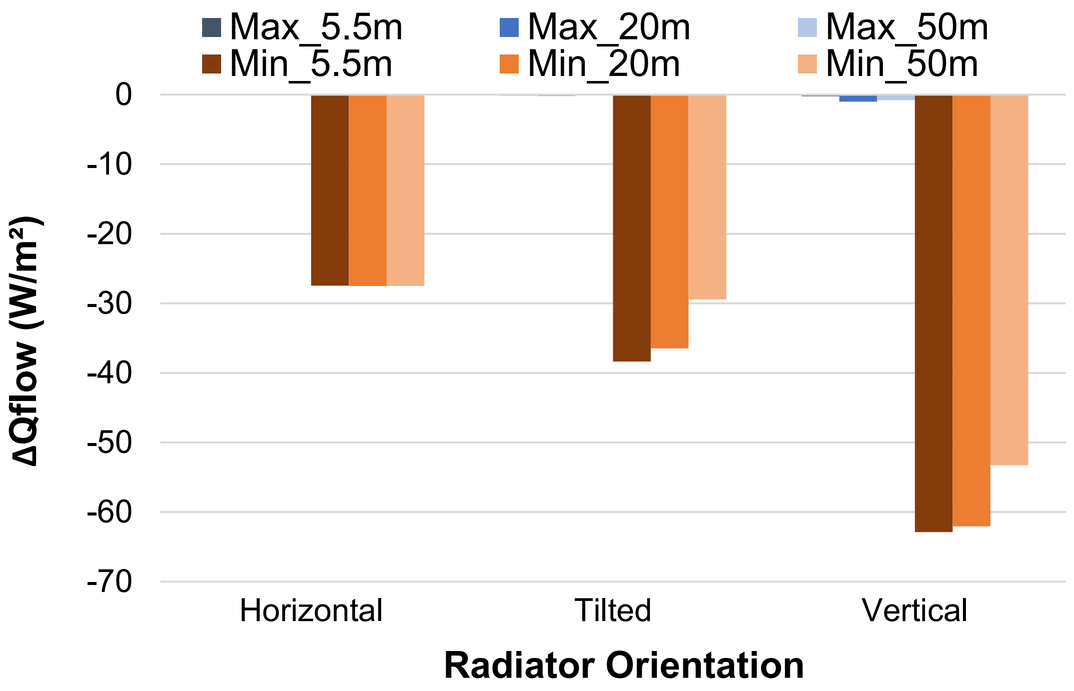

(2) Delta: Crater, Max & Min Heat Rejection (single panel)

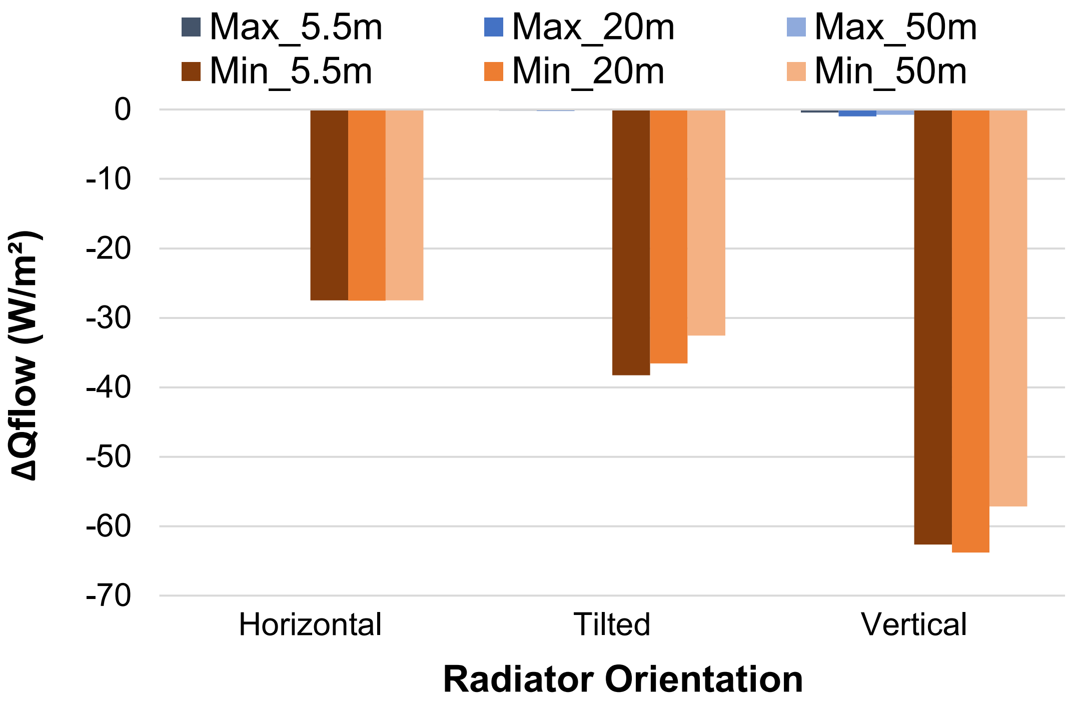

HLS

Study Findings

- **Small craters and sloped features of medium sized craters, that are not typically captured in Lunar surface meshes, <u>do not</u> impart meaningful thermal impacts upon Lunar landers when compared to a flat surface plane**
  - Impact magnitude may be different for a smaller and more thermally sensitive asset (e.g., astronaut suit), not analyzed here

- **Radiator orientation (horizontal, tilted, vertical) significantly impacts heat rejection capability in the hot case**
  - Hot case heat rejection capability radiator orientation trend: Horizontal > Tilted > Vertical
  - Hot case radiator height impacts on heat rejection capability are negligible
  - Cold case performance is similar for all analyzed radiator orientations and heights

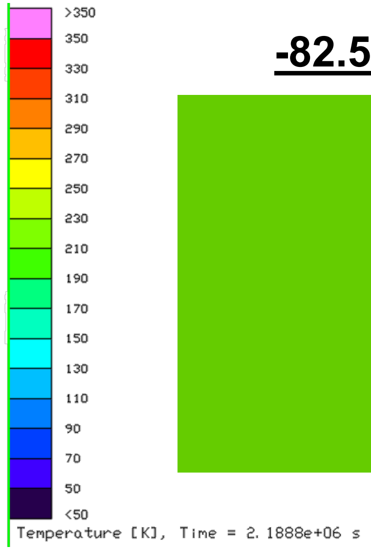

<u>-82.5ºS Flat Surface, 5.5m lander height</u>

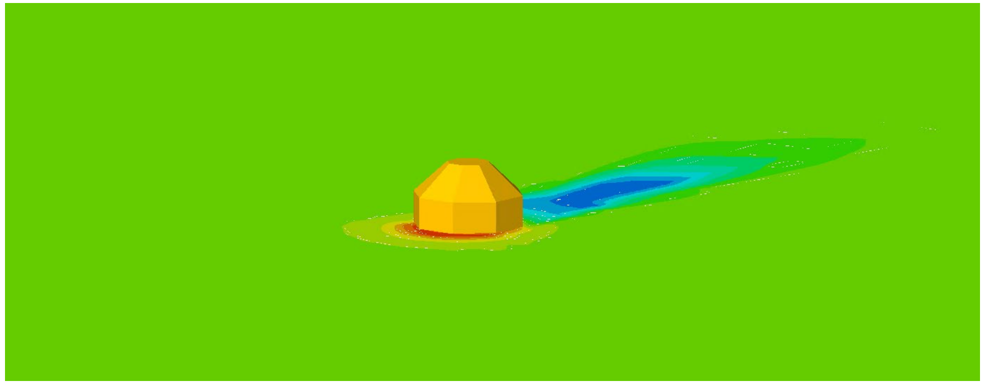

<u>-82.5ºS Crater Surface, 5.5m lander height</u>

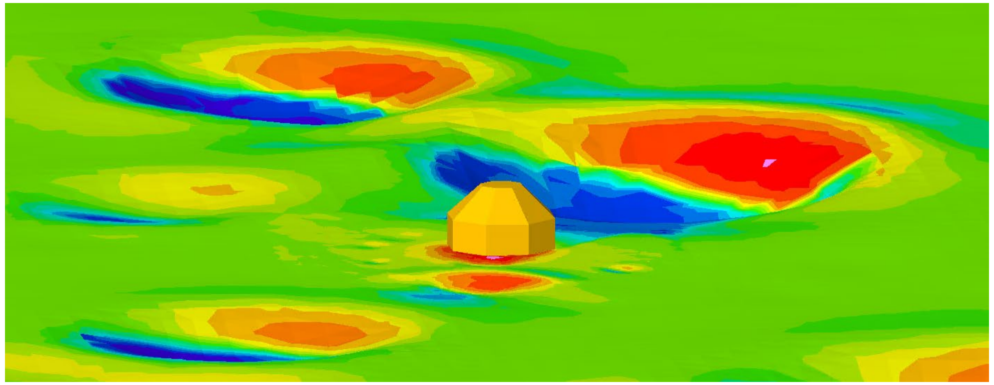

HLS

References

[1] W. Birmingham, G. Schunk, and B. Evans, "Lunar Latitude and Terrain Radiator Sensitivity Study," 2024. [Online]. Available: https://ntrs.nasa.gov/api/citations/20240010276/downloads/Lunar_Latitude_and_Terrain_Radiator_Sensitivity_V2.pdf

[2] W. Birmingham, W. Grier, and L. Erickson, "Lunar South Pole Terrain Effects on Radiator Performance," Nasa.gov, Aug. 04, 2025. https://ntrs.nasa.gov/citations/20250007546 (accessed Nov. 29, 2025).

[3] B. D. Hamill, R. G. Schunk, and L. R. Erickson, "Human Landing System Lunar Thermal Analysis Guidebook," Jan. 2021, Available: https://ntrs.nasa.gov/citations/20210010030

[4] F. B. Leahy, "SLS-SPEC-159, Cross-Program Design Specification for Natural Environments (DSNE)," Oct. 2021. Available: https://ntrs.nasa.gov/citations/20210024522

[5] "Horizons System," Available: https://ssd.jpl.nasa.gov/horizons/

[6]T.-Y. Park, J.-J. Lee, J.-H. Kim, and H.-U. Oh, "Preliminary Thermal Design and Analysis of Lunar Lander for Night Survival," International Journal of Aerospace Engineering, vol. 2018, pp. 1–13, Oct. 2018, doi: https://doi.org/10.1155/2018/4236396.

[7] E. J. Foote, D. A. Paige, M. K. Shepard, J. R. Johnson, and S. Biggar, "The bidirectional and directional hemispheric reflectance of Apollo 11 and 16 soils: Laboratory and Diviner measurements," Icarus, vol. 336, p. 113456, Jan. 2020, doi: 10.1016/j.icarus.2019.113456.

[8] A. R. Vasavada et al., "Lunar equatorial surface temperatures and regolith properties from the Diviner Lunar Radiometer Experiment," Journal of Geophysical Research: Planets, vol. 117, no. E12, p. n/a-n/a, Apr. 2012, doi: https://doi.org/10.1029/2011je003987.

[9] P. O. Hayne et al., "Global Regolith Thermophysical Properties of the Moon From the Diviner Lunar Radiometer Experiment," Journal of Geophysical Research: Planets, vol. 122, no. 12, pp. 2371–2400, Dec. 2017, doi: https://doi.org/10.1002/2017je005387.

[10] R. Woods-Robinson, M. A. Siegler, and D. A. Paige, "A Model for the Thermophysical Properties of Lunar Regolith at Low Temperatures," Journal of Geophysical Research: Planets, vol. 124, no. 7, pp. 1989–2011, Jul. 2019, doi: https://doi.org/10.1029/2019je005955

[11] L. Erickson, C. Gomez, B. Hamill, and G. Schunk, "Lunar Thermal Analysis Guidebook: Thermo-physical and Optical Properties of Lunar Regolith." Available: https://ntrs.nasa.gov/api/citations/20220013412

[12] "Fireflyspace.com, 2025. https://fireflyspace.com/wp-content/uploads/2025/01/BGM1-Component-Graphic-vJan14-2025a.png

[13] "NOVA-C | Intuitive Machines," Intuitive Machines, 2024. https://www.intuitivemachines.com/nova-c

[14] "NASA's Apollo 11 Lunar Module (Basic Facts)," Apollo11Space, Dec. 08, 2019. https://apollo11space.com/nasas-apollo-11-lunar-module-basic-facts/

[15] Wikipedia Contributors, "Blue Moon (spacecraft)," Wikipedia, Nov. 21, 2025.

[16] Astralytical, "SpaceX's Starship vs Blue Origin's Blue Moon: Who's landing first?," Substack.com, Mar. 18, 2024. https://astralytical.substack.com/p/spacexs-starship-vs-blue-origins (accessed Nov. 29, 2025).

[17] "NeoGeographyToolkit/synthterrain: Tools for the generation of synthetic planetary terrain," GitHub, Mar. 27, 2025. https://github.com/NeoGeographyToolkit/synthterrain (accessed Nov. 29, 2025).

[18] A. Liounis et al., "Tutorial on LuNaMaps Developed Tools andProcesses for Mapping the Lunar Surface," Nasa.gov, Oct. 07, 2024. https://ntrs.nasa.gov/citations/20240012330 (accessed Nov. 29, 2025).

[19] C. Restrepo et al., "Technology Transfer Plan: LuNaMaps Project," Nasa.gov, Oct. 07, 2024. https://ntrs.nasa.gov/citations/20240012328 (accessed Nov. 29, 2025).

@NASAARTEMIS